S_N2 Reaction Rate Enhancement by β-cyclodextrin at the Liquid/Liquid Interface

*John J. Karnes and Ilan Benjamin**

Department of Chemistry and Biochemistry, University of California-Santa Cruz, Santa Cruz, CA, 95064.

ABSTRACT

An inverse phase transfer catalyst typically enhances the rate of biphasic reaction by bringing the water-insoluble reactant from the organic to the aqueous phase. We use the empirical valence bond (EVB) approach to obtain reaction free energy profiles for a model S_N2 reaction inside the β-cyclodextrin (β-CD) cavity at the water/1-bromooctane interface and in bulk water, to show that a significant rate enhancement is taking place at the liquid/liquid interface rather than in the bulk. By examining several solvent-solute structural and energetic properties, we demonstrate that the rate enhancement when the reaction takes place inside the cavity at the interface is primarily due to limited accessibility of interfacial water molecules, which results in destabilization of the reactants. Greater accessibility of water molecules when the catalyst is in the bulk stabilizes the reactants and does not lead to rate enhancement despite the significant hydrophobicity of the cavity's interior.

I. INTRODUCTION

Many chemical reactions of interest take place between reactants that are soluble in dissimilar phases, for example when a water-soluble polar molecule reacts with a non-polar, oil-soluble molecule.[1] Since the reaction requires close contact between the reactants, this reaction can take place only at the water/oil interface, which, due to mass transport and geometrical constraints, significantly limits its rate. Phase transfer catalysts can enhance the rate by shuttling the polar reactant into the organic ("oil") phase (normal Phase Transfer Catalysis, PTC)[1–4] or by transferring the non-polar reactant to the aqueous phase (Inverse Phase Transfer Catalysis, IPTC).[5–7]

A well-known example of an inverse phase transfer catalyst is β-cyclodextrin (β-CD). The β-CD molecule is a cyclic sugar consisting of 7 glucose units, whose general geometry resembles a truncated cone.[8] Figure 1 provides a simulation snapshot and a cartoon representation for reference. The glucose hydroxyl groups surround both the large and small openings, resulting in an interesting electrostatic profile where the outside of the molecule has considerable polar character and its inner cavity is nonpolar. Because of this, β-CD readily forms host/guest complexes with nonpolar molecules.

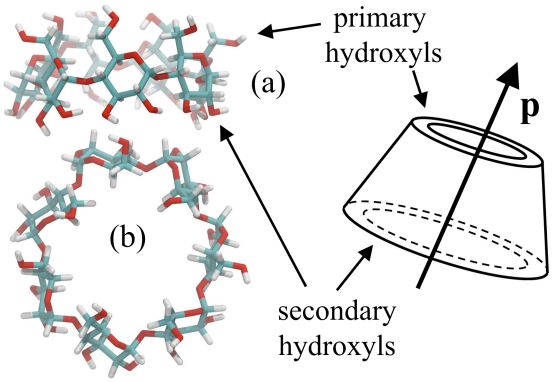

Figure1. Representative structures of β-CD shown using "licorice" models, viewed perpendicular to (a) and looking into the pore (b). The general morphology of β-CD resembles a truncated cone (c).

An important class of reactions subject to PTC or IPTC are nucleophilic substitution reactions (S_N2). The rate of S_N2 reactions is incredibly sensitive to the local environment surrounding the reacting species, reported in cases to decrease by 20 orders of magnitude when moving from the gas phase to bulk water.[9–11] These reactions are also faster by many orders of magnitude when carried out in nonpolar solvent instead of water. The surrounding polar solvent molecules provide greater stabilization to the charge-localized reactant and product states than to the more diffused charge of the transition state (TS), significantly increasing the energy gap between reactant/product and TS, thus increasing the barrier to reaction.

An interesting example of an S_N2 reaction catalyzed by β-CD that provides the motivation for our work is $CN^- + CH_3(CH_2)_7Br \rightarrow CH_3(CH_2)_7CN + Br^-$ carried out at the interface between 1-bromooctane and water by Triponov and Nikiforov,[12] who found that addition of β-CD increases the rate of the reaction by (only) a factor of 8. This result is puzzling given the significant enhancement in the rate expected when the reactants are located in non-polar environments like the interior cavity of β-CD. This reaction is also unusual because each interfacial molecule of the non-polar phase is a potential reactant, thus reducing the need for mass transport to the interface.

We recently reported molecular dynamics simulation results on the stability of β-CD/1-bromooctane host/guest complexes in bulk 1-bromooctane, bulk water, and at the interface of

these two immiscible solvents.[13] We found little to no energetic barrier to host/guest complexation/dissociation in the organic phase or at the liquid/liquid interface but a substantial barrier to dissociation when in the aqueous phase. This host/guest interaction supports the idea of a phase transfer mechanism: the surface-active β-CD can easily form an inclusion complex with 1-bromooctane when at the interface. The complex diffuses to bulk water where the guest is effectively 'locked' in place and where it is most likely to be exposed to the nucleophilic attack by CN^-. The product/β-CD complex diffuses to the interface where it dissociates and the cycle continues.

However, the precise catalytic function and phase transfer mechanism of β-CD in this and other systems remain unclear. An alternative mechanism that has been suggested is that the surface-active β-CD brings the organic guest molecule to the interface, exposing the reactive moiety to the aqueous phase at the interface, and allows the product species to diffuse away (as opposed to shuttling the guest into the aqueous phase.)[14,15] Our energy/stability studies are consistent with both mechanisms, since exchange of the 1-bromooctane guest at the interface toward the aqueous phase was seen to be quite facile, suggesting that β-CD may remain at the interface and serve primarily to orient the 1-bromooctane reactive site in a manner that facilitates reaction with species in the adjacent phase as suggested.

The IPTC mechanism describes catalysis in the context of assisted mass transfer, where the role of the phase transfer catalyst is to reduce the physical distance between reactants and allow chemical reaction. However, it is possible that the IPTC catalyst also functions as a more traditional catalyst, and alters the electronic configuration of the chemical reaction along the

reaction coordinate and lowers the energetic barrier to reaction. Indeed, β-CD's impact on chemical reactions has been well studied.[7,8,16–21] One interesting application of β-CD host/guest complexation involves reactive species with multiple reactive sites. In some cases, the geometry and polarity of β-CD allow it to form a host/guest complex that sterically hinders reaction at one of these sites, effectively shielding the 'guest' site and directing the chemical reaction toward the site with which β-CD does not complex.[19] The IPTC mechanism in a β-CD catalyzed system like those studied by Triponov and Nikiforov[12] may also benefit from the local volume excluded by the β-CD host in addition to enhanced mass transfer between the phases. If the β-CD host serves to exclude water from the reactive site, it may result in decreased stabilization of the reactant/product states, effectively reducing the reaction barrier. The purpose of the present work is to more closely investigate these factors and focus on the chemical reaction in this IPTC system.

To investigate this idea, we revisit the 1-bromooctane/water/ β-CD system and include a chemical reaction in our simulation model. The experimental work on which we base our studies involves the S_N2 reaction between 1-bromooctane and an aqueous nucleophile, but in these initial studies we focus our attention on a simpler system, the symmetric S_N2 reaction $Cl^- + CH_3Cl \rightarrow ClCH_3 + Cl^-$. This reaction has served as a benchmark system for the theoretical and computational study of solvent effects on chemical reaction thermodynamics and dynamics.[9,22–25] Implementation and use of this model reaction to probe the complex solvation environments in the β-CD IPTC system allows us to compare the results to the large body of theoretical and computational studies performed on this reaction. The free energy profile of this benchmark system has been studied in a wide range of molecular-level simulations in a variety of solvents of varying polarity, quantifying the impact of solvent polarity on the reaction barrier.

We have previously reported studies of this reaction at the water-air interface, in small clusters of water within bulk organic solvent, and at the interface of two immiscible liquids.[23,26–28] Here we briefly summarize two main points from our previous work that capture some of the insights relevant to this IPTC system. First, the presence of only a few molecules of water in an otherwise nonpolar environment has a dramatic effect on the free energy profile of this reaction. Molecules in the first solvation shell dominate the interaction potential between solute and solvent and are therefore mostly responsible for the stabilization of the product/reactant states. Since this solvation shell typically consists of only a few solvent molecules, the significant impact of a single, polar solvent molecule within an otherwise nonpolar system may retard the rate of reaction by several orders of magnitude. Second, surprisingly, the rate of the benchmark reaction at the immiscible water/oil interface is slower than in bulk water. This is due to the fact that at the liquid/liquid interface the aqueous phase provides similar stability of the highly charge-localized reactant and product states as it provides in bulk water. However, the interaction between the delocalized charges of the transition state and the surrounding solvents is quite weak and similar to that provided by the organic phase. The reduced stability of the transition state and the enhanced stability of the reactants (and products) results in a larger net barrier to reaction.[27]

The proximity of the β-CD host molecule to the S_N2 reactive center makes the system considerably more complex since the β-CD may significantly alter the local solvation environment in ways besides simply limiting solvent molecule access to the reactive center. The structural fluctuations and localized protrusions of one phase into the adjacent phase inherent to the liquid/liquid interface significantly influence (and accompany) mass transfer at and between the phases. At the water/oil interface β-CD preferentially orients so that one of its circular openings is parallel to the interface, with the hydroxyl groups at that opening participating in

hydrogen bonds with interfacial water molecules. This ring of hydrogen bonds should serve to isolate the β-CD pore from interfacial fluctuations, effectively causing the interfacial β-CD pore region to resemble a nonpolar membrane cavity.

To quantify the influence of the β-CD host molecule on the benchmark S_N2 reaction, this work examines the free energy profile when the reactive system is located within the β-CD cavity. We consider both energetic and structural factors, the interaction potential and arrangement of molecules that surround the reaction site, to understand the influence of the β-CD host molecule. The results are discussed in the context of existing studies of the benchmark S_N2 reaction and their implications toward understanding inverse phase transfer catalysis. The rest of this work is organized a follows: Section II describes the details of our reactive molecular dynamics simulations and free energy calculations. Section III presents the results of these simulations and relevant analyses. Section IV summarizes and outlines future work.

II. SYSTEMS AND METHODS

A. Non-reactive force fields and simulation details

This work considers a model S_N2 reaction in several different solvent environments, including bulk liquids, the interface between two immiscible liquids, and within the pore of β-CD. The composition and geometries of these systems are listed in Table 1. The nonreactive force fields used to represent water, 1-bromooctane, and β-CD have been described recently[13] and are summarized here for convenience. Intermolecular potentials are the pairwise sum of Lennard-Jones and Coulomb terms,

$$u_{ij}(r) = 4\varepsilon_{ij}\left[\left(\frac{\sigma_{ij}}{r}\right)^{12} - \left(\frac{\sigma_{ij}}{r}\right)^{6}\right] + \frac{q_i q_j}{4\pi r \varepsilon_0} \quad (1)$$

where r is the distance between atom centers i and j. Standard Lorentz-Berthelot combining rules are used to generate mixed interaction parameters. Our water model is a version of the flexible SPC force field[29] with intramolecular potentials as described by Kuchitsu and Morino.[30] The oil phase (1-bromooctane) consists of a charged head group (q_{Br} = -0.22)[31] and an OPLS-UA alkane tail.[32] The united-atom 1-bromooctane model is employed to reduce computational complexity. Adding parameters beyond the charged head group and electrically neutral alkane tail would not provide any interesting additional physical insight to this work. The β-CD molecule is a fully-flexible, all-atom representation with parameters taken from the AMBER99SB-ILDN force field.[33] Since this work is focused on the detailed effect of the β-CD on a model S_N2 reaction, its impact when functioning as a 'molecular-reactor,[19,20]' we use the all-atom representation. All molecular dynamics simulations are performed using our in-house code that uses the velocity Verlet algorithm and a time-step of 0.5 fs to integrate the laws of motion.[34] All simulations are performed at 298 K. System snapshots are obtained using Visual Molecular Dynamics (VMD.)[35]

Table 1. Composition and Sizes of Simulated Systems

system	n_{BrOct}	n_{H_2O}	$n_{\beta\text{-CD}}$	x (Å)	y (Å)	z (Å)
A	384	0	0	60.0[a]	60.0[a]	60.0[a]
B	0	999	0	39.11[a]	39.11[a]	39.11[a]
C	509	2030	0	45.0	45.0	300.0
D	0	2104	1	50.0[a]	50.0[a]	50.0[a]
E	610	2400	1	50.0	50.0	300.0

[a]Dimensions refer to the cube which encloses systems with truncated octahedral symmetry.

B. The empirical valence bond (EVB) model

To model the S_N2 reaction we use an EVB approach similar to the model first introduced by Warshel and coworkers.[9,36] The EVB model describes a chemical reaction as a mixture of diabatic states, whose condensed-phase interaction potentials are equal to the gas-phase potentials plus the interaction between each state and its surrounding solvent (and the β-CD when present). The EVB method can describe the changing electronic configuration along the reaction coordinate while being computationally inexpensive enough to allow the simulation of a reactive system within large, condensed-phase molecular systems. We refer the reader to a previously published, detailed discussion of our implementation[23] and other works that present the EVB approach with greater depth.[37,38] Here we briefly summarize the EVB model, focusing on the components relevant to the analysis presented later in this work.

We use the simplest approach to consider the symmetric S_N2 reaction $Cl^- + CH_3Cl \rightarrow CH_3Cl + Cl^-$ and assume that only two orthonormal valence states contribute to the total wavefunction: $\Psi_1 = Cl^- + CH_3Cl$ and $\Psi_2 = CH_3Cl + Cl^-$.[22,23]

$$\Psi = c_1\psi_1 + c_2\psi_2, \ \langle \psi_i | \psi_j \rangle = \delta_{ij} \tag{2}$$

The total Hamiltonian is

$$\hat{H} = \begin{pmatrix} H_{11}(\mathbf{r}_i, \mathbf{r}_d, \mathbf{r}_s) & H_{12}(r_1, r_2, \theta) \\ H_{21}(r_1, r_2, \theta) & H_{22}(\mathbf{r}_i, \mathbf{r}_d, \mathbf{r}_s) \end{pmatrix} \tag{3}$$

where H_{11} and H_{22} are the Hamiltonians for the diabatic states Ψ_1 and Ψ_2:

$$H_{11} = E_k + H_{11}^0(r_1, r_2, \theta) + U_{ss}(\mathbf{r}_s) + U_{si}(\mathbf{r}_s, \mathbf{r}_i) + U_{sd}(\mathbf{r}_s, \mathbf{r}_d), \quad (4)$$

which includes E_k, the kinetic energy of all atoms and H_{11}^0, the gas phase Cl^- ion – CH_3Cl molecule interaction potential. U_{ss}, U_{si}, and U_{sd} represent the solvent–solvent, solvent–Cl^- (ion), and solvent–CH_3Cl (dipole) interaction potentials. Due to the symmetric nature of the reaction, H_{22} is of identical form and involves only changing the indices of the Cl atom centers. The off-diagonal terms in Equation 3, H_{12} and H_{21}, are the electronic coupling terms used by Hynes and coworkers[22,39]

$$H_{12} = -QS(r_1)S(r_2) \quad (5)$$

where $S(r)$ is the overlap integral for the σ orbital formed by the carbon 2p and chlorine 3p orbitals, determined using the approximations of Mulliken et. al.[40] Q is a parameter fitted so that the correct gas-phase potential energy surface is obtained, set to 678.0 kcal/mol. Diagonalization of the Hamiltonian in eq. 3 gives rise to the ground state adiabatic Hamiltonian H_{ad} used to propagate the reactive classical trajectories.

We define a simple, geometric reaction coordinate to be the difference between the Cl and CH_3 atom centers, $\xi = r_1 - r_2$, where the reaction coordinate ξ is precisely zero at the transition state (TS) because of the symmetric nature of the reaction studied in this work.

To quantify the degree with which the solvent stabilizes the reactants vs. the products, we define a "solvent coordinate" $s(\xi)$ at each value of ξ by considering the solute-solvent interaction potential's contribution to the energy gap $H_{11} - H_{22}$:

$$H_{11} - H_{22} = \Delta H^0 + s, \quad (6)$$

where ΔH^0 is the energy gap between the gas-phase diabatic states. Note that at the transition state $\langle s \rangle = 0$.

C. Reaction free energy profile calculations

We calculate the free energy profile of the model S_N2 reaction along the reaction coordinate ξ using umbrella sampling with overlapping windows and an applied biasing potential. Our implementation may be formally described by starting with the definition

$$\begin{aligned} W(\xi) &= -k_B T \ln \langle \delta(r_1 - r_2 - \xi) \rangle \\ &= -k_B T \ln \frac{\int \delta(r_1 - r_2 - \xi) e^{-H_{ad}/k_B T} \, d\Gamma}{\int e^{-H_{ad}/k_B T} \, d\Gamma} = -k_B T \ln P(\xi) \end{aligned} \tag{7}$$

where k_B is the Boltzmann constant and δ is the Dirac delta function. The free energy profile $W(\xi)$ over the interval $[\xi_0, \xi_N]$ may be calculated by dividing the interval into N overlapping subintervals, where the value of ξ in a window j is constrained to $[\xi_{j-1}, \xi_j]$ by window potentials applied as a function of r_1 and r_2. The resulting set of overlapping $W_j(\xi)$ are stitched together by adding a constant C_j that minimizes the difference between the overlapping regions of $W_{j-1}(\xi)$ and $W_j(\xi)$. To improve sampling statistics and accelerate the exploration of phase space a biasing potential is added to the adiabatic Hamiltonian,

$$H_{ad}^b = H_{ad} + U_b(\xi) \tag{8}$$

where U_b is a function of ξ and is of the form

$$U_b(\xi) = Ae^{-\alpha\xi^2} - Be^{-\beta|\xi|} . \tag{9}$$

The parameters A, α, B, and β are chosen so that $U_b(\xi)$ approximates $W(\xi)$. The reported free energy profile is given by

$$W(\xi) = -k_B T \ln\left\langle \ln \delta(r_1 - r_2 - \xi)\right\rangle_b - U_b(\xi) \tag{10}$$

noting that the ensemble average $\langle \ldots \rangle_b$ is obtained using the Hamiltonian modified by the applied biasing potential, H_{ad}^b.

In this work all data is presented as a function of the reaction coordinate ξ and is obtained by sampling overlapping windows along ξ as mentioned above. Each window is 0.5 Å wide and overlaps the neighboring window by 0.2 Å. 1 ns of trajectory data is collected within each window.

III. RESULTS AND DISCUSSION

A. Reaction in bulk liquids

As a useful reference we first consider our benchmark reaction in bulk of the two liquids. Figure 2a shows the potential of mean force W along the reaction coordinate ξ for the $Cl^- + CH_3Cl \rightarrow ClCH_3 + Cl^-$ reaction in bulk water, 1-bromooctane, and in vacuum. The large differences in the free energy profiles and the activation free energies $\Delta A^{\ddagger}$ in these three systems is due to the changing solvation environment of the reactive system along ξ. The polar solvents stabilize the reactant and product states much more than the reaction's transition state due to the greater charge separation and magnitude in the reactant/product states than in the transition state. As a result, the barrier to the reaction increases by 10 kcal/mol in 1-bromooctane relative to vacuum and by an additional 15 kcal/mol in water relative to 1-bromooctane. We refer the reader

to our earlier, more extensive survey and discussion of this reactive system in solvents of increasing polarity.[23] We also draw attention to the ion-dipole minima at $\xi = \pm 1.5$ Å. These minima are due to the electrostatic attraction between the Cl^- and the electrophilic end of the CH_3Cl dipole and are most prominent in vacuum and in non-polar solvent environments. With increasing solvent polarity and thus stabilization of the product/reactant states, the ion-dipole minima diminish, effectively vanishing when in an aqueous environment.[23] The free energy barrier is defined as the difference between the free energy at $\xi = -\infty$ (free energy of reactants) and the maximum height of the free energy profile at the transition state ($\xi = 0$.)

The equilibrium value of the solvent coordinate s_{eq} in each solvent is shown in Figure 2b. As described in Equation 6, s_{eq} is the contribution of solvent-solute interaction energy to the energy gap between the two diabatic states, $H_{11} - H_{22}$, and serves as a useful quantitative probe of the reaction's local environment. The dependence of s_{eq} on ξ illustrates the solvent-solute coupling. The magnitude of s_{eq} when ξ is far from the transition state describes the solvation energy contribution to the barrier height. The slope of $s_{eq}(\xi)$ near the transition state describes the rate of preferential solvation of the reactant/product states as the charge separation increases with increasing $|\xi|$.[23,41]

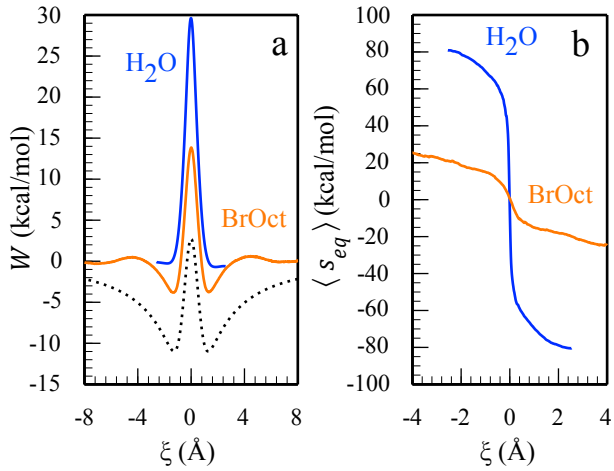

Figure 2. (a) Potential of mean force W and (b) equilibrium value of the solvent coordinate s_{eq} along the reaction coordinate ξ for the reaction $Cl^- + CH_3Cl \rightarrow CH_3Cl + Cl^-$ in bulk water, 1-bromooctane, and in vacuum.

The structure of local solvent molecules surrounding the reaction may be described as a function of ξ by considering the radial distribution function

$$g_{vl}(r) = \frac{1}{\eta_c}\left\langle \sum_{i=1}^{N} \delta(r - r_i) \right\rangle \tag{11}$$

where v is the Cl^-, CH_3, or Cl atom center, l is the representative atom center in the solvent molecule, and r_i is the distance between the atomic centers v and l. δ is the Dirac delta function, N is the total number of pair distances, and the normalization constant η_c is chosen so that $g_{vl}(r \rightarrow \infty) = 1$. For water, the oxygen molecule is the representative atom center and for 1-bromooctane the united atom CH_2 adjacent to the Br atom (αC) is selected as the representative atom center. Since this αC united atom bears a partial positive charge, its arrangement around the Cl^- will contribute most significantly toward the solvent-solute interaction potential and thus to s_{eq}. The

local solvent structure around the ion, $g_{vl}(r)$, may be expressed as a function of ξ by extracting the maximum value of $g_{vl}(r)$ (g_{max}) from trajectories obtained during the umbrella sampling of the reaction, one data point obtained for each overlapping 0.5 Å-wide window along ξ. The results of these calculations for the reaction $Cl^- + CH_3Cl \rightarrow ClCH_3 + Cl^-$ in bulk water and bulk 1-bromooctane are shown in Figure 3. Three curves are obtained for each solvent for $v = Cl^-, CH_3$, and Cl. The two panels in Figure 3 correspond to solvents of very different size and polarity yet show a similar behavior. We may describe these curves by moving along the reaction coordinate ξ from left to right. As the Cl^- nucleophile (green curve) approaches CH_3Cl, the ordering of its solvation shell rapidly decreases near the transition state at $\xi = 0$ Å. In similar fashion, the solvation shell around the Cl leaving group (red curve) tightens and becomes more ordered as the charge on the leaving group increases immediately after crossing the TS and moving toward + ξ. The two panels are similar in overall shape but with significantly different g_{max} magnitudes. This difference largely reflects the normalization of $g_{vl}(r)$ to unit bulk density and the size difference between the two solvent molecules. If we define the population of the first solvation shell by integrating the first peak of $g_{vl}(r)$ the number of the solvent molecules surrounding the Cl ions is more similar, 7.7 water molecules and 6.2 1-bromooctane αC atom centers. In the case of both solvents, the CH_3 atom center (blue curve) shows little enhanced solvation, even in the regions near $\xi = 0$, where the values of g_{max} change dramatically for both the nucleophile and leaving group.

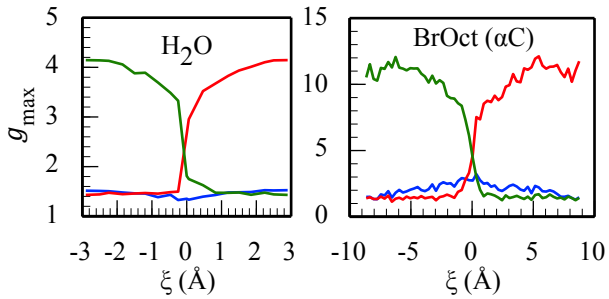

Figure 3. Solvation of the atom centers in the EVB reactive system. Curves represent the maximum value of $g_{vl}(r)$ for the respective atom center surrounding solvent molecules: the Cl^- nucleophile (green), the leaving Cl^- (red), and the CH_3 united atom (blue). The central solvent atoms are the water oxygen (left panel) and the 1-bromooctane α-carbon (right).

B. Reaction in aqueous host/guest complex

We next consider the benchmark reaction carried out within the interior of the β-CD cavity in bulk water. To help decide on the precise location for the reactants, we invoke our previous work where we examined the host/guest stability of the β-CD/1-bromooctane complex in bulk water, bulk 1-bromooctane and at the liquid/liquid interface.[13] Stability studies of the host/guest complex in bulk water showed that the minimum-free energy (most-favored) location of the 1-bromooctane guest corresponds to having the reactive site (the carbon adjacent to the bromine atom, αC) near the hydroxyl groups at either opening and the alkane tail within the β-CD pore. Guided by this observation, we insert the benchmark system at these two energetically favored positions and obtain potential of mean force curves along the reaction coordinate ξ in bulk water, while the reactants' center of mass is constrained to the given location. A third curve is also

obtained by constraining the benchmark S_N2 reaction to the 'center' of the β-CD pore. While this location is not physically relevant to the 1-bromooctane/β-CD host/guest complex, we include this in our effort to fully probe the impact of β-CD on this benchmark S_N2 reaction. All β-CD – reactive system constraints involve restricting the center of mass of the benchmark system with a windowing potential perpendicular to the β-CD molecular vector **p** shown in Figure 1c (and therefore parallel to the β-CD pore openings). The cartoon in the upper right of Figure 4 illustrates the positions of the benchmark reaction for each corresponding free energy profile. The planar constraints, as distances from the β-CD center of mass along **p,** are 4.20 ± 0.25 Å at the small opening, -3.90 ± 0.25 Å at the large opening, and -1.0 ± 0.5 Å for the 'center' of the pore.

Figure 4a shows free energy profiles for the aqueous $Cl^- + CH_3Cl \rightarrow CH_3Cl + Cl^-$ reaction/β-CD host/guest complex at various guest locations compared to the reaction in bulk water (blue curve). Surprisingly, all three host/guest configurations show a similar reaction barrier as the one in bulk water with no β-CD present. This is also reflected in the nearly identical variation of the solvent coordinate as a function of the reaction coordinate in the different locations shown in Figure 4b. Evidentially the hydrophobicity of the β-CD interior must be counterbalanced by the water molecules remaining in the cavity and near the mouth of the pore as well as by the existence of many OH groups around each pore opening. All these species are able to provide enhanced stabilization of the reactants and product states that is only slightly reduced from that in bulk water while at the same time providing significantly less stabilization of the transition state than that in bulk water. This is similar to what has been observed in studies of this benchmark S_N2 system at water interfaces[26,27] and in water clusters within nonpolar solvents.[28] Figure 5 is a qualitative sketch of free energy diagrams, showing the relative stability of the

transition state and products/reactants in different environments. In the β-CD pore, like at the neat liquid/liquid interface, the increase in barrier height is mostly due to reduced stabilization of the transition state.

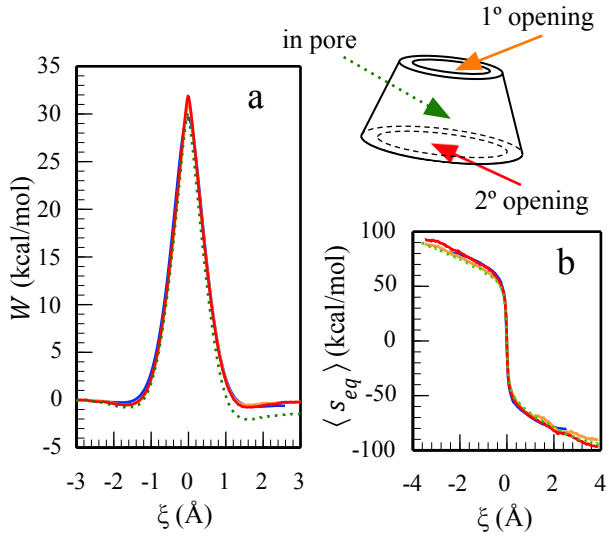

Figure 4. Free energy profiles (a) and equilibrium solvent coordinate values (b) for the reaction $Cl^- + CH_3Cl \rightarrow CH_3Cl + Cl^-$ in bulk water (blue) and as guest in β-CD pore in water at three positions: at the small, primary hydroxyl opening (orange), at the larger, secondary hydroxyl opening (red), and near the β-CD's center of mass (green, dotted). The cartoon in the upper right shows the approximate location of the reactive system as guest in the β-CD molecule.

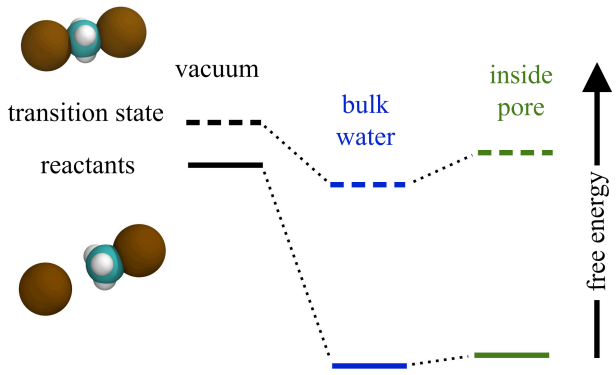

Figure 5. A cartoon depicting (not to scale) the free energy of the transition state (dashed lines) and the reactants (solid lines) in different environments.

Support for the above explanation is provided by examination of the local structure around the S_N2 reaction. This can again be described by considering $g_{max}(\xi)$, the maximum value of $g_{vl}(r)$ in each umbrella-sampling window along ξ. However, to appropriately account for the presence of β-CD, the ability of its hydroxyl groups to solvate the S_N2 system must also be considered. As a first approximation we again apply Equation 11 to construct pair distribution functions but count both water and β-CD hydroxyl group oxygens as the relevant solvent moiety (l) when calculating $g_{vl}(r)$. This assumption is reasonable since the β-CD hydroxyl hydrogens are assigned partial charges within +0.01 e of our water model's hydrogen charge of +0.41 e, therefore providing similar stability to the negatively charged species in the benchmark system. Comparing the host/guest g_{max} plots in Figure 6 to the corresponding analysis performed in bulk water (Figure 3), it is seen that the reactant/product hydration shell populations are only slightly larger in the aqueous system without β-CD. The peak values of g at the transition states are smaller when the S_N2 system is within the β-CD molecule. The net effect of the cavity is to stabilize the reactants (and products) to a degree that is almost the same as in bulk water while to stabilize the transition state to a degree that is much less than in bulk water.

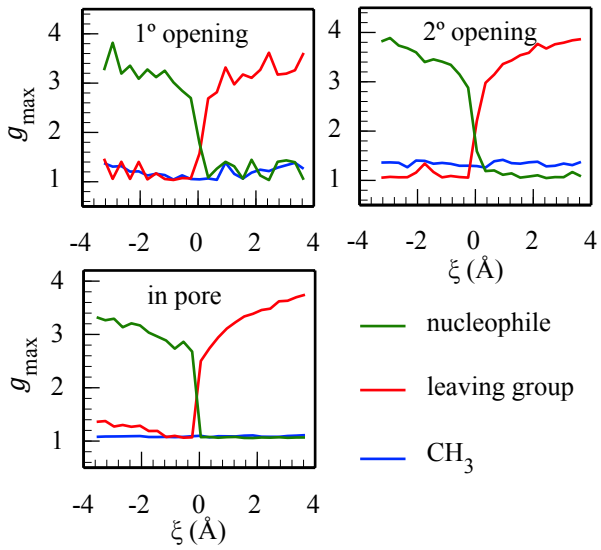

Figure 6. The maximum value of $g_{vl}(r)$ along ξ describes the solvation of the β-CD complexed reactive system atom centers in an aqueous system. Each panel represents the reactive system at a different location within the β-CD host molecule. Following ξ from left to right, the curves correspond to the Cl nucleophile (green), the CH_3 reaction center (blue), and the Cl leaving group (red). All g_{max} values represent the total solvation of the reactive system by water and β-CD hydroxyl groups (see text for details).

We conclude this section by noting the small asymmetry in the PMF when the reaction takes place in the middle of the β-CD pore. In this location the Cl-CH_3-Cl system is approximately locked in an orientation that gives rise to different local hydration for the two Cl atoms, which results in breaking the symmetry of the reaction. This is evident from comparing the peak values of g for the two Cl atoms in Figure 6. While the two curves describing the hydration of the nucleophile and the leaving groups at the two openings of the cavity are symmetrical, the

corresponding curves are clearly non-symmetrical when the reaction takes place in the center of the pore. Interestingly, each curve is similar to one of the curves at each of the two openings (compare the 'in pore' green curve with the green curve at the 1º opening and the 'in pore' red curve with the red curve at the 2º opening).

C. Reactions at the liquid/liquid interface

We next consider the more complicated situation when the host/guest complex is located at the liquid/liquid interface. We first define a simple nomenclature adapted from one introduced by Zheng et. al.[42] In our simulations, the z-axis is normal to the interface, with the Gibbs Dividing Surface (GDS) located at approximately $z = 0$ Å, the 1-bromooctane phase located in the region of $z > 0$ Å, and the aqueous phase at $z < 0$ Å. The surface-active β-CD molecule is located near the GDS, with its center of mass in the organic phase and one of the circular pore openings parallel to the interface (the vector **p** defined in Figure 1 is perpendicular to the interface). To simplify and clarify the discussion of the host/guest system at the liquid interface, we define the system where the β-CD is at the interface with the large opening near the GDS and the small opening pointing toward $+z$ (toward the bulk organic phase) as Δ or "up." Similarly, when the β-CD small opening is at the GDS and the large opening toward $+z$, we shall refer to this system as ∇ or "down." A cartoon schematic of this nomenclature is included in the upper right of Figure 7.

In each host/guest configuration the reactive system is confined to the minimum energy position of the reactive site in a corresponding β-CD/1-bromooctane host/guest complex as determined in our preceding work.[13] The constraint on the position of the S_N2 system uses the same form as the

constraints applied in the β-CD/S_N2/water system described in Section III.C, with the S_N2 system's center of mass confined to a plane parallel to the pore openings and separated from the β-CD center of mass by 4.20 ± 0.25 Å at the small opening and -3.90 ± 0.25 Å at the large opening. The arrows in the cartoon in Figure 7 indicate the approximate location of the S_N2 system center of mass at the liquid/liquid interface and the colors of the arrows correspond to the respective free energy profiles.

Figure 7a shows the free energy profile for the $Cl^- + CH_3Cl \rightarrow ClCH_3 + Cl^-$ reaction at the neat interface (red curve) and when the reactive system is guest within the β-CD molecule in the Δ (blue) and ∇ (green) positions. At the neat interface, the reaction barrier is approximately 32.2 kcal/mol, noticeably greater than in bulk water. This increase in barrier height at the interface due to diminished stabilization of the transition state has been described in earlier sections and discussed in detail in our previous work.[27] The two interfacial host/guest systems (blue and green) have nearly indistinguishable profiles, which again suggests that the difference between the two openings has little impact on the hosted reactive system. However, unlike in the aqueous systems in Section III C, the interfacial host/guest systems have a lower barrier to reaction than the corresponding reactive system without the β-CD host molecule. The magnitudes of the host/guest reaction barriers at the interface are 29.8 kcal/mol for the Δ configuration and 28.8 kcal/mol for the ∇ configuration, both substantially lower than the value obtained at the neat interface.

This result has important consequence in regard to the IPTC reaction: When β-CD hosts the reaction at the interface, it acts as a conventional catalyst by lowering the barrier to reaction relative to the corresponding system without β-CD present. This catalytic function of β-CD is

provided by its shielding of the reactive system from some interfacial water molecules, resulting in less stabilization of the reactant and product states. If the reduction in barrier height were due to β-CD weakly binding to or locally distorting the reactive system itself to lower the reaction barrier, we should see a similar effect in the host/guest system in bulk water, an effect not seen in Figure 4a.

The values of $s_{eq}(\xi)$ for the interfacial systems in Figure 7b agree with the free energy profile calculations. Moving away from the transition state ($\xi = 0$ Å) all curves rapidly increase in magnitude as charge separation increases. Away from the transition state the host/guest systems both have smaller magnitude values of s_{eq} than the neat interfacial system.

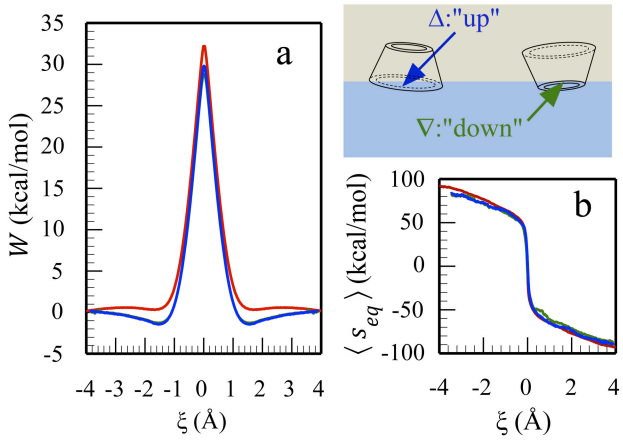

Figure 7. Free energy profile (a) and equilibrium value of the solvent coordinate (b) for the S_N2 system at the liquid/liquid interface. The blue and green curves represent the reactive system as guest within β-CD in the Δ ("up") and ∇ ("down") orientations, the red curve is the neat interface. The cartoon on the upper right shows the location of the reactive system and β-CD in

each system. The light brown background represents the 1-bromooctane phase and the aqueous phase is light blue.

In Figure 8 we again utilize $g_{max}(\xi)$ to describe the stabilization of the benchmark reactive system by the surrounding solvent. The top two panels describe solvation of the bare solute system at the liquid/liquid interface, the top left panel of Figure 8 refers to solvation by water and the top right refers to solvation by 1-bromooctane, where the αC is again used as the atom center of reference due to its partial positive charge. These two panels describe a phenomenon reported earlier when this benchmark reactive system is observed at the immiscible water/organic interface. When away from the transition state, the charge-bearing Cl atom center is solvated by water and the CH_3Cl 'dipole' resides in the organic phase, solvated predominantly by the 1-bromooctane.

The bottom two panels of Figure 8 show $g_{max}(\xi)$ for the interfacial host/guest Δ and ∇ configurations. Like in the case of the host/guest system in bulk water, the solute-solvent pair distribution functions contain the sum of both water and β-CD hydroxyl oxygen atoms as the solvent.

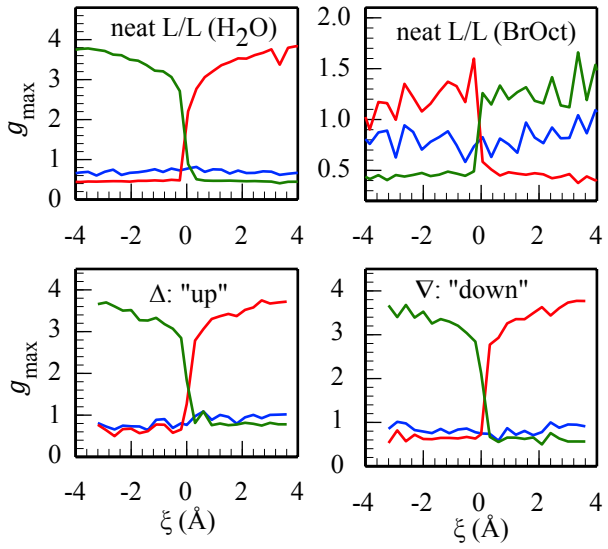

Figure 8. Solvation of the atom centers in the model S_N2 system at the liquid/liquid interface. The top panels represent the reactive system at the neat interface, solvated by water (left) and 1-bromooctane (right). The bottom panels represent the total solvation of the reactive system by water and β-CD hydroxyl groups (see text for details).

IV. CONCLUSIONS

We have studied the effect of complexation with β-CD in various solvent environments on the benchmark symmetric S_N2 reaction $Cl^- + CH_3Cl \rightarrow ClCH_3 + Cl^-$ by molecular dynamics simulations to gain insight into the mechanism of Inverse Phase Transfer Catalysis. In bulk water the reaction is almost unaffected by the complexation of the reactants with β-CD. Despite the hydrophobic nature of the β-CD cavity, water molecules remaining in the cavity and near the opening, along with the β-CD OH groups, provide a hydration environment close to bulk water. At the immiscible liquid/liquid interface the formation of an inclusion complex with β-CD reduces the barrier height relative to the reaction at the neat interface. This is due to the fact that at the interface the β-CD molecule resides mostly in the organic phase, with nonpolar species preferentially populating the pore. The β-CD host molecule partially restricts access of interfacial water molecules to the guest S_N2 system, resulting in a slightly reduced stabilization of the reactant/product states.

This work suggests that β-CD may act as both a conventional catalyst (reducing the energetic barrier to reaction along the reaction coordinate) and phase transfer catalyst (facilitating mass transfer of one reactant to an adjacent, immiscible phase). It provides a qualitative explanation for the rate enhancement observed experimentally for the reaction $CN^- + CH_3(CH_2)_7Br \rightarrow CH_3(CH_2)_7CN + Br^-$ at the water/1-bromooctane interface.[12] Work is in

progress to develop a new EVB model that considers this specific reaction. The presence of an alkane tail directly adjacent to the reactive center (inside the cavity) may, upon first consideration, suggest additional local dehydration of the reactive site, further reducing the energetic barrier to reaction. However, as determined by earlier studies,[13] the 1-bromooctane reactive site typically resides at the outer edge of the β-CD pore. Therefore the alkane tail may have a negligible impact on the magnitude of stabilization provided by nearby solvent molecules. Insight gained from the present work will be useful for isolating the different factors that may (or may not) influence the rate in this more complex system.

ASSOCIATED CONTENT

The Supporting Information is available free of charge on the ACS publications website at DOI: …

Representative simulation snapshots of systems listed in Table 1 (PDF)

AUTHOR INFORMATION

Corresponding Author

* Email: benjamin@chemistry.ucsc.edu; Telephone: 831-459-3152.

ACKNOWLEDGMENT

This work is supported by the National Science Foundation through grant CHE-1363076.

REFERENCES

(1) Mąkosza, M.; Fedoryński, M. Phase Transfer Catalysis. *Catal. Rev.* **2003**, *45*, 321–367.

(2) Starks, C. M.; Liotta, C. L.; Halpern, M. E. Phase-Transfer Catalysis: Fundamentals I. In *Phase-Transfer Catalysis*; Springer Netherlands, 1994; pp. 23–47.

(3) Halpern, M. Phase-Transfer Catalysis. In *Ullmann's Encyclopedia of Industrial Chemistry*; Wiley-VCH Verlag GmbH & Co. KGaA, 2000.

(4) Ooi, T.; Maruoka, K. Recent Advances in Asymmetric Phase-Transfer Catalysis. *Angew. Chem. Int. Ed.* **2007**, *46*, 4222–4266.

(5) Mathias, L. J.; Vaidya, R. A. Inverse Phase Transfer Catalysis. First Report of a New Class of Interfacial Reactions. *J. Am. Chem. Soc.* **1986**, *108*, 1093–1094.

(6) Boyer, B.; Hambardzoumian, A.; Roque, J.-P.; Beylerian, N. Reaction in Biphasic Water/Organic Solvent System in the Presence of Surfactant: Inverse Phase Transfer Catalysis versus Interfacial Catalysis. *Tetrahedron* **2000**, *56*, 303–307.

(7) Monflier, E.; Tilloy, S.; Castanet, Y.; Mortreux, A. Chemically Modified β-Cyclodextrins: Efficient Supramolecular Carriers for the Biphasic Hydrogenation of Water-Insoluble Aldehydes. *Tetrahedron Lett.* **1998**, *39*, 2959–2960.

(8) Takahashi, K. Organic Reactions Mediated by Cyclodextrins. *Chem. Rev.* **1998**, *98*, 2013–2034.

(9) Hwang, J. K.; King, G.; Creighton, S.; Warshel, A. Simulation of Free Energy Relationships and Dynamics of S_N2 Reactions in Aqueous Solution. *J. Am. Chem. Soc.* **1988**, *110*, 5297–5311.

(10) Chandrasekhar, J.; Smith, S. F.; Jorgensen, W. L. SN2 Reaction Profiles in the Gas Phase and Aqueous Solution. *J. Am. Chem. Soc.* **1984**, *106*, 3049–3050.

(11) Ingold, C. K. *Structure and Mechanism in Organic Chemistry*; 2nd ed.; Cornell University: Ithaca, NY, 1969.

(12) Triponov, A. Z.; Nikiforov, T. T. Cyclodextrins as Phase-Transfer Catalysts in a Nucleophilic Displacement Reaction. *J. Mol. Catal.* **1984**, *24*, 15–18.

(13) Karnes, J. J.; Benjamin, I. Structure and Dynamics of Host/Guest Complexation at the Liquid/Liquid Interface: Implications for Inverse Phase Transfer Catalysis. *J. Phys. Chem. C* **2017**, *121*, 4999–5011.

(14) Sieffert, N.; Wipff, G. Importance of Interfacial Adsorption in the Biphasic Hydroformylation of Higher Olefins Promoted by Cyclodextrins: A Molecular Dynamics Study at the Decene/Water Interface. *Chem. Eur. J.* **2007**, *13*, 1978–1990.

(15) Sieffert, N.; Wipff, G. Adsorption at the Liquid-Liquid Interface in the Biphasic Rhodium Catalyzed Hydroformylation of Olefins Promoted by Cyclodextrins: A Molecular Dynamics Study. *J. Phys. Chem. B* **2006**, *110*, 4125–4134.

(16) Banerjee, A.; Sengupta, P. K. Encapsulation of 3-Hydroxyflavone and Fisetin in β-Cyclodextrins: Excited State Proton Transfer Fluorescence and Molecular Mechanics Studies. *Chem. Phys. Lett.* **2006**, *424*, 379–386.

(17) Sen, S.; Sukul, D.; Dutta, P.; Bhattacharyya, K. Slow Solvation Dynamics of Dimethylformamide in a Nanocavity. 4-Aminophthalimide in β-Cyclodextrin. *J. Phys. Chem. A* **2001**, *105*, 10635–10639.

(18) Mukhopadhyay, M.; Banerjee, D.; Mukherjee, S. Proton-Transfer Reaction of 4-Methyl 2,6-Diformyl Phenol in Cyclodextrin Nanocage. *J. Phys. Chem. A* **2006**, *110*, 12743–12751.

(19) Barr, L.; Dumanski, P. G.; Easton, C. J.; Harper, J. B.; Lee, K.; Lincoln, S. F.; Meyer, A. G.; Simpson, J. S. Cyclodextrin Molecular Reactors. *J. Incl. Phenom. Macrocycl. Chem.* **2004**, *50*, 19–24.

(20) Easton, C. J. Cyclodextrin-Based Catalysts and Molecular Reactors. *Pure Appl. Chem.* **2009**, *77*, 1865–1871.

(21) Szejtli, J. Introduction and General Overview of Cyclodextrin Chemistry. *Chem. Rev.* **1998**, *98*, 1743–1754.

(22) Mathis, J. R.; Bianco, R.; Hynes, J. T. On the Activation Free Energy of the Cl– + CH3Cl S_N2 Reaction in Solution. *J. Mol. Liq.* **1994**, *61*, 81–101.

(23) Benjamin, I. Empirical Valence Bond Model of an S_N2 Reaction in Polar and Nonpolar Solvents. *J. Chem. Phys.* **2008**, *129*, 74508.

(24) Gertner, B. J.; Whitnell, R. M.; Wilson, K. R.; Hynes, J. T. Activation to the Transition State: Reactant and Solvent Energy Flow for a Model SN2 Reaction in Water. *J. Am. Chem. Soc.* **1991**, *113*, 74–87.

(25) Sun, L.; Hase, W. L.; Song, K. Trajectory Studies of SN2 Nucleophilic Substitution. 8. Central Barrier Dynamics for Gas Phase Cl- + CH3Cl. *J. Am. Chem. Soc.* **2001**, *123*, 5753–5756.

(26) Nelson, K. V.; Benjamin, I. A Model S_N2 Reaction "on Water" Does Not Show Rate Enhancement. *Chem. Phys. Lett.* **2011**, *508*, 59–62.

(27) Nelson, K. V.; Benjamin, I. A Molecular Dynamics-Empirical Valence Bond Study of an S_N2 Reaction at the Water/Chloroform Interface. *J. Phys. Chem. C* **2010**, *114*, 1154–1163.

(28) Nelson, K. V.; Benjamin, I. A Molecular Dynamics/EVB Study of an S_N2 Reaction in Water Clusters. *Chem. Phys. Lett.* **2010**, *492*, 220–225.

(29) Berendsen, H. J. C.; Postma, J. P. M.; Van Gunsteren, W. F.; Hermans, J. In *Intermolecular Forces*; Pullman, B., Ed.; D. Reidel: Dordrecht, 1981; p. 331.

(30) Kuchitsu, K.; Morino, Y. Estimation of Anharmonic Potential Constants. II. Bent XY_2 Molecules. *Bull. Chem. Soc. Jpn.* **1965**, *38*, 814–824.

(31) Müller, T.; Werblowsky, T. L.; Florio, G. M.; Berne, B. J.; Flynn, G. W. Ultra-High Vacuum Scanning Tunneling Microscopy and Theoretical Studies of 1-Halohexane Monolayers on Graphite. *Proc. Natl. Acad. Sci. U. S. A.* **2005**, *102*, 5315–5322.

(32) Jorgensen, W. L.; Madura, J. D.; Swenson, C. J. Optimized Intermolecular Potential Functions for Liquid Hydrocarbons. *J. Am. Chem. Soc.* **1984**, *106*, 6638–6646.

(33) Lindorff-Larsen, K.; Piana, S.; Palmo, K.; Maragakis, P.; Klepeis, J. L.; Dror, R. O.; Shaw, D. E. Improved Side-Chain Torsion Potentials for the Amber ff99SB Protein Force Field. *Proteins Struct. Funct. Bioinforma.* **2010**, *78*, 1950–1958.

(34) Verlet, L. Computer "experiments" on Classical Fluids. I. Thermodynamical Properties of Lennard-Jones Molecules. *Phys. Rev.* **1967**, *159*, 98–103.

(35) Humphrey, W.; Dalke, A.; Schulten, K. VMD: Visual Molecular Dynamics. *J. Mol. Graph.* **1996**, *14*, 33–38.

(36) Warshel, A.; Weiss, R. M. An Empirical Valence Bond Approach for Comparing Reactions in Solutions and in Enzymes. *J. Am. Chem. Soc.* **1980**, *102*, 6218–6226.

(37) Warshel, A. *Computer Modeling of Chemical Reactions in Enzymes and Solutions*; Wiley, 1991.

(38) Kamerlin, S. C. L.; Warshel, A. The Empirical Valence Bond Model: Theory and Applications. *Wiley Interdiscip. Rev. Comput. Mol. Sci.* **2011**, *1*, 30–45.

(39) Juanos i Timoneda, J.; Hynes, J. T. Nonequilibrium Free Energy Surfaces for Hydrogen-Bonded Proton-Transfer Complexes in Solution. *J. Phys. Chem.* **1991**, *95*, 10431–10442.

(40) Mulliken, R. S.; Rieke, C. A.; Orloff, D.; Orloff, H. Formulas and Numerical Tables for Overlap Integrals. *J. Chem. Phys.* **1949**, *17*, 1248–1267.

(41) Gertner, B. J.; Bergsma, J. P.; Wilson, K. R.; Lee, S.; Hynes, J. T. Nonadiabatic Solvation Model for S_N2 Reactions in Polar Solvents. *J. Chem. Phys.* **1987**, *86*, 1377–1386.

(42) Zheng, X.; Wang, D.; Shuai, Z.; Zhang, X. Molecular Dynamics Simulations of the Supramolecular Assembly between an Azobenzene-Containing Surfactant and α-Cyclodextrin: Role of Photoisomerization. *J. Phys. Chem. B* **2012**, *116*, 823–832.

TOC Graphic